μNRIT-2.5 - A New Optimized Microthruster Of Giessen University

IEPC-2009-174

D. Feili[1], B. Lotz, St. Bonnet, B. K. Meyer, H.W. Loeb
Justus Liebig University Giessen, Heinrich-Buff-Ring 16, 35392 Giessen

and

N. Puetmann[2]
Deutsches Zentrum für Luft- und Raumfahrt e. V. (DLR), Königswinterer Strasse 522-524, 53227 Bonn

Some future scientific space missions will need highly precise microthrusters for position and attitude control, repositioning and transportation to the operation locus. Rf-ion engines of the RIT-type, running with an electrodeless discharge and exhausting the inert gas Xenon, are potential candidates within the entire thrusting range of 5μN to 5mN.

While the 4cm engine RIT-4 is already under industrial D&Q program, Giessen University, developed, a half-sized thruster μNRIT-2.5 under DLR contract. The advanced 2.5cm breadboard model is equipped with a 37-holes grid system, and it showed a thrusting range between 50μN and nearly 600μN. By reducing the number of beamlet apertures, 5μN-levels may be obtained. At a thruster mass of only 210g and a power consumption of about 30W, the μNRIT-2.5 engine fulfils mission requirements.

I. Introduction

Early in 2004, a program of scaling-down of the successful 10cm-engine RIT-10 (flown onboard EURECA and ARTEMIS) started at Giessen University. A more than 30 yrs old research work on a 4cm engine revived[1], and scaling laws of the RIT-type have been established in order to shorten the microthruster development procedure[2].

First, a new laboratory prototype μNRIT-4 has been built that could be equipped alternatively with 151 beamlet apertures (for full-power operation) and 19 or 7 holes (for diagnostics), respectively. The tests have been done in a refurbished Giessen facility "Big Mac" (2.2m^3 chamber volume, 24,000ltr/s cryopumping speed).[2]

In spring 2005, the engine was tested at ESTEC Noordwijk.[3] Then, EADS-Astrium started a D&Q program on an engineering model RIT-4 EM with 37 grid borings under ESA/ ESTEC sponsorship.[4] The related duration tests have been carried out in a new Giessen facility "R2D2" (4.5m^3 chamber volume, 24,000ltr/s cryopumping speed). In the meantime, diagnostic tests with the Giessen μNRIT-4 LP have been continued.[5]

Already in 2005, a laboratory 2cm rf-microthruster μNRIT-2 with 7 beamlet borings in the grid system was built, optimized and tested at Giessen.

In order to cover the fine-microthrusting range of 50μN to 500μN, this type has been enlarged for 2.5cm of ionizer diameter which allowed drilling 37 beamlet borings into the two grid system. By using all the experiences gained in the meantime, an advanced breadboard microthruster μNRIT-2.5 has been built in the institute's workshop, and the performance was mapped in the Big Mac-facility.[7] For this, an elegant data acquisition software has been developed, too.[7]

II. Basic Advantages and Development Tasks

Due to the following special features of rf-engines, a microthrusting application of them seems to be promising:

(1) The non-aggressive, volatile inert gas Xenon serves as the propellant
(2) The electrodeless discharge stands not opposite to a mechanical scaling-down.
(3) Furthermore, the absence of discharge electrodes avoids all related lifetime problems.
(4) The high-voltage grid system enables sufficiently high specific impulses, even if the propellant efficiency would be rather poor.

[1] Head of EP Group, Giessen University, Email: Feili@uni-Giessen.de.

[2] DLR, Satellites' subsystems. Postfach 30 03 64, 53183 Bonn, E-mail: Norbert.Puettmann@DLR.de

(5) The modest beam densities (being the consequence of space-charge limitation in the accel region) avoid a too strong miniaturization of the engine even if very small thrust levels should be generated.
(6) Despite of these a-priori advantages, a deliberated design and careful optimizations must care for a competitive position of the RIT-type.
(7) As up to 16 microthrusters must be installed on relatively small spacecrafts, the mass of each engine, its power and propellant consumption should be kept within acceptable limits.
(8) The required lifetime must be guaranteed.
(9) Thrust noise, thrust accuracy and stepping ability must meet the mission specifications.

III. Design Guide Lines

The mode of working of a gridded rf-ion thruster of the RIT-type has been repeatedly reported.[2, 8,9,10] Thus, we can confine ourselves to the critical topics connected with the miniaturization of rf-ion thrusters. They are ruled by scaling laws.[2, 6, 10]

3.1 Ionizer Design

Caused by the energy accumulation process of the ionizing discharge electrons, the first scaling law suggests that the rf-frequency ω and the discharge pressure p must be increased when the ionizer radius R decreases:

$$\omega \sim p \sim 1/R \qquad \text{Equ.1}$$

In the case of *optimum discharge frequency*, ω_{opt}, the plasma condition of Equ.1 is overlapped by external effects like eddy currents in structural parts, etc. Thus, we get the experimental data collated in Table 1. Note that the ω-curve shows a broad maximum and no sharp resonance.

The experimentally found *optimum discharge pressure* p_{opt} follows roughly Equ.1, too. The higher pressure data of microthrusters- compared e.g. to RIT-10- reduce not only the *propellant efficiencies* η_m and the specific impulses I_{sp}, but enlarge also the charge exchange rates inside the grid systems, lowering their lifetime expectation.

To keep these effects within acceptable limits, the *propellant injector* of µNRIT-2.5 has been redesigned: Due to the induction law and verified by discharge plasma diagnostics[2], the induced electrical eddy field and the temperature of the discharge electrons have their maximum near the ionizer walls. Therefore, it is advantageous to inject the gas into the ionizer in axial direction at the circumference of the screen grid, using the counter-current principle, too. The comparison with the standard gas distributers placed at the ionizer top of RIT-4 and RIT-10 shows that about 25% of neutral gas losses could be saved by the new design (see Table 1).

Another drawback of any microengine- compared to larger thrusters of the same type- is the increasing ratio of the ionizer surface vs. its volume. For a cylindrical vessel this ratio amounts to 2/R + 1/l (with l = ionizer length). As the ion production takes place inside the ionizer, whereas the ambipolar recombination losses appear at the ionizer surface, the surface-to-volume-ratio should be small. Otherwise, the *ion production costs* w_i would increase with 1/R (see Table 1), lowering the *power efficiency* η_e, too.

There exist two measures to keep this size penalty within reasonable limits:

First, the ionizer should have an *optimum length* l_{opt} which is a compromise between a small surface-to-volume ratio and a sufficient long duration of stay of the neutral atoms in the discharge vessel to have a chance of being ionized. This scaling law has been verified experimentally for several rf-ion sources and working gases:2, 6, 10

$$l_{opt} = (2R)^{\alpha}\, with\, \alpha(Xe) = 0.66; l_{opt} \text{ and R in cm} \qquad \text{Equ.2}$$

The second way to reduce the ionizer surface is to replace the cylindrical discharge vessel by a semispherical one. This new *ionizer shape* has been first introduced with the RIT-15 engine[11] and then adapted for RIT-22 and the rf-microthruster µNRIT-2.5.[7, 10] Experiments showed a rf-power saving between 15% and 25% and a corresponding increase of η_e.

The *ion current density* j_i, offered by the discharge plasma to the grid system, depends both on the plasma density α and the electron temperature T_e: [2, 8,9,10]

$$j_i = 0.6065 q_i n \cdot \sqrt{\frac{kT_e}{m_i}} \qquad \text{Equ.3}$$

(q_i = mean ion charge, k = Boltzmann's constant, m_i = mean ion mass). Plasma density n and electron temperature T_e depend on the two discharge operation parameters, namely the rf-power P_{REG} and the propellant flow rate $\dot{V}$ (or the discharge pressure p). In the discharge characteristics, i.e. the P_{REG} vs. $\dot{V}$ diagrams, the j_i = const curves show the known hyperbolic shape.[8]

The working parameters P_{REG} and $\dot{V}$ should be chosen in such a way that the total thruster efficiency $\eta_m \eta_e$ keeps its maximum. In addition, the electron temperature T_e should not be too high because it rules the positive *plasma potential* V_P that cares for equal electron and ion currents to the wall (see above):

$$V_P = 9.85 \cdot \frac{kT_e}{2e} \quad \text{for Xenon} \qquad \text{Equ.4}$$

Usually, the electron temperature kT_e is in the order of 5eV which generated plasma potential of about 25V. However, if T_e and V_P are significantly higher, the sputter threshold of the screen grid could be surpassed. The geometry of the rf-coil may contribute to such a hazardous case.

Table 1. Comparison between RIT-10 EVO, RIT-4 and RIT-2.5 equipped with grid systems of maximum open area and running at nominal thrust; the beamlet geometries are the same; the ionizer pressure was calculated by the neutral gas flow rate and the gas conductivity of the grid system.

	RIT-10 EVO	µNRIT-4	µNRIT-2.5
number of beamlets	1483	151	37
open area of the screen grid, %	53.5	34.1	21.4
nominal thrust, mN	25	3.5	0.5
optimum frequency, MHz	~1	~2	~3
optimum ionizer pressure, 10^{-3} Torr	0.41	0.84	1.0
optimum ionizer length, cm	4.6	2.5	1.8
ion production costs, eV per ion	472	769	2438
power efficiency, %	79.6	69.5	42.6
propellant efficiency, %	80.2	66.2	49.1

3.2 Grid System Design

Besides of the diameter, the *standard grid geometry* of RIT-10 EVO, RIT-15, RIT-22 and µNRIT-4 has been adapted for µNRIT-2.5, too (see Table 2). Within optimum beamlet focusing condition, the microthruster may be operated between 0.8kV and 2.1kV of positive high voltage.

Another feature of RIT-microthrusters- in comparison with the larger rf-engines- is the decreasing *open area ratio* of the first grid (see Table 1), which contributes also to the increased ion production costs. This is caused by the fact that the periphery of the grid system should be free from borings, because the plasma density decreases strongly near the ionizer walls.[2]

Whereas the RIT-10 was equipped with a three-grid system, i.e. with a closed decel grid to protect the accel grid against backstreaming ions, the RIT-15 and RIT-22 engines used two-grid systems with an open, grounded decel ring. This was done because of simplification and cost reduction, and it worked without lifetime problems.

However, in the case of microthrusters with their increased pressure data (in the discharge, between the grids, and also behind), a *closed third grid* should be installed to shield the second grid against charge exchange ions generated at the thruster exit.

IV. Construction of the µNRIT-2.5 Engine

Following, the design guide lines, the 2.5 cm rf-microthruster has been constructed and built in the institute's workshop at the beginning of 2008.

Fig. 1: Photo of the 2.5cm rf-microthruster µNRIT-2.5 of Giessen University.[7, 10]

Figs. 1 shows a photo of the engine.

The *ionizer vessel* is made (in the laboratory model) of quartz, and it has an optimized shape with an inner diameter (at the basis) of 2.5cm and a length of 2.25cm. Together with the frequency (2.9MHz), the ionizer/ rf-coil geometry has been optimized by simulation with the "Maxwell" computer program.[7]

The isolator of the *propellant feed system* is made of ceramics and filled with quartz sand. It is placed aside the ionizer vessel. 12 gas micronozzels are arranged at the outer circumference of the screen grid.

Actually, i.e. prior to lifetime testing, a two-grid system (molybdenum/ graphite) with 37 beamlet borings in a hexagonal structure is used.

Both the optimized ionizer vessel and the gas injector system are essential improvements with respect to the µNRIT-4 microthruster.

The µNRIT-2.5 engine has an outer diameter of 6cm and a length of 5.8cm. Its mass is only 210g.

V. Performance of the µNRIT-2.5 Engine

Following some calibration and functional tests, a first nine months performance mapping campaign was done to be reported in the following.

All tests have been performed in Giessen's facility "Big Mac". Fig.4 shows the microthruster installed inside.

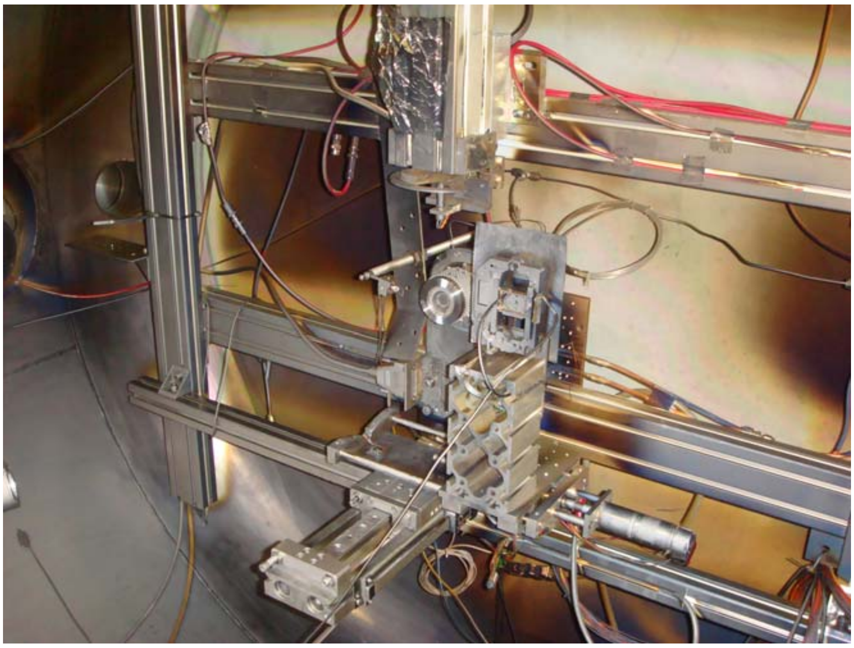

Fig. 2: Microthruster µNRIT-2.5 installed on a test platform in the facility "Big Mac".[7, 10]

5.1 Discharge Characteristics

The basic behaviour of any rf-discharge is characterized by the extractable ion current IBeam (as the parameter) as function of the two operation quantities, namely the required rf-power P_{REG} and the gas flow rate $\dot{V}$.

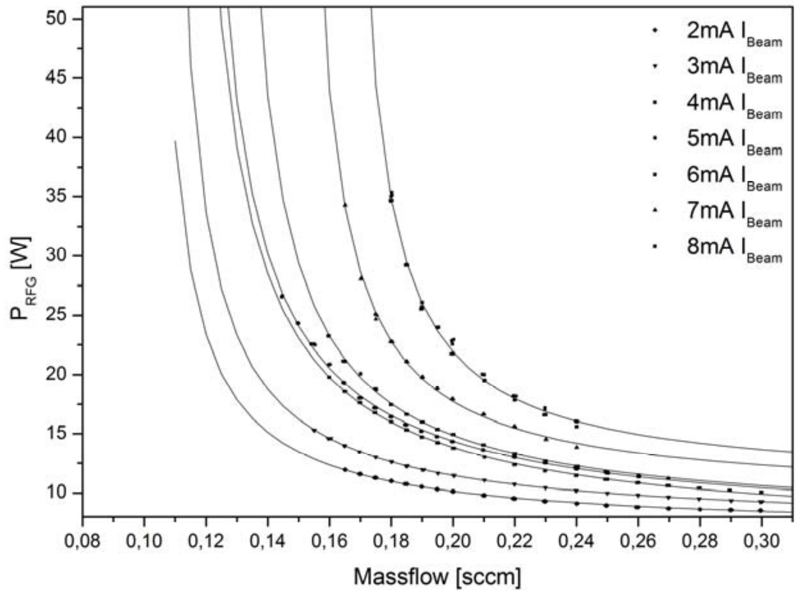

Fig. 3: Extracted beam current (2mA to 8mA as the parameter) of µNRIT-2.5 as function of the required rf-generator power PRFG and the propellant flow rate MFC.[7, 10]

Fig.3 shows the hyperbola-like characteristics IBeam ($P_{REG}, \dot{V}$) of µNRIT-2.5. Obviously, a certain beam current may be generated either by a relatively high rf-power together with a low gas consumption or vice versa or around the vertex of the hyperbola that gives the maximum total efficiency $\eta_m\eta_e$.

It may be interesting to compare the related curves of the 2.5cm Giessen microthruster with the 4cm engine RIT-4 that has 37 extraction holes, too.[4]

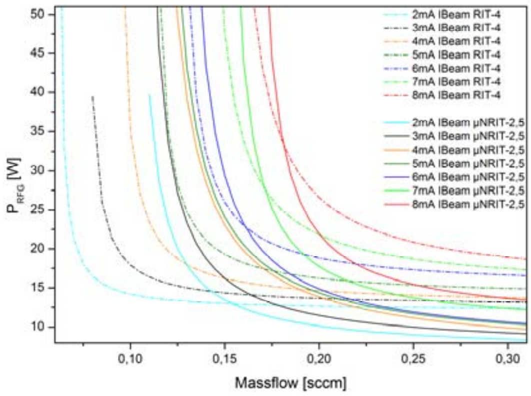

Fig. 4: Comparison of the discharge characteristics IBeam (P_{RFG}, $\dot{V}$) of the Giessen µNRIT-2.5 engine[7, 10] and of the 4cm microthruster RIT-µx of EADS-Astrium;[4] both engines are equipped with a two-grid system having 37 beamlet borings.

Fig.6 shows that the larger thruster saves propellant especially in the low thrusting range (due to the reduced discharge pressure; see Table 1), whereas the smaller engines saves rf-power especially at higher $\dot{V}$ operation (due to the smaller ionizer surface; see above).

5.2 Grid System Characteristics

It is well known that an effective grid system must not only accelerate the flowing in plasma ions (Equ.3), but also focus the beamlets. Fig.5 shows the range of *optimum focusing*, i.e. the beam voltage (vs. the beam current) for which the accel drain current could be kept within 0.1mA (including charge exchanged ions). Beyond the upper borderline and underneath the lower borderline, the over- and under-focused case provokes too high drain currents, respectively.

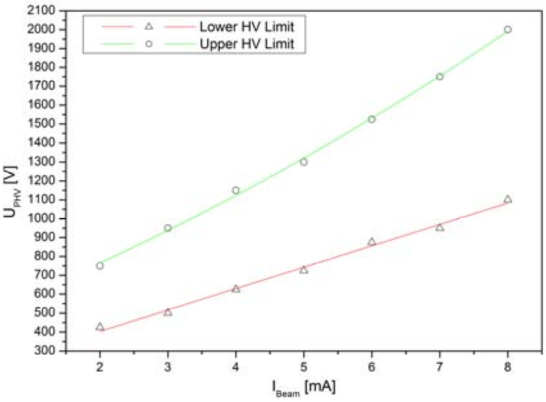

Fig. 5: Range of the positive high voltage U_{PHV} (with upper and lower borders) in which the optimum focusing of the beamlets are maintained vs. the beam current IBeam.[7, 10]

The graph gives also the *throttling range* if the positive high voltage should be kept constant. E.g. for U_{PHV} = 1.25kV we get an extractable beam current between 4.25mA and 8.5mA, i.e. a thrusting range between 245µN and 490µN.

The negative high voltage U_{NHV}, applied to the accel grid, has been kept constant at -100V (up to 3mA of beamcurrent) and -125V (for IBeam > 3mA). Experiments showed that these voltages are sufficient to repel backstreaming electrons.

We mention that the accelerator voltage should not be higher than the named minimum to keep the sputter rate of charge exchange ions,generated in the grid system, within acceptable limits.

5.3 Overall performance

As a benefit of the (otherwise disadvantageous) high ionizer pressure (see Table 1), the discharge can easily be ignited even without drawing neutralizer electrons into the discharge vessel as usual.

By using a beam control loop, the thrust could be kept very constant. Fig. 8 shows a *thrust stepping* test. Table 3 gives the µNRIT-2.5 *performance data* (without neutralizer).

Table 2: Throttling performance of the Giessen microthruster µNRIT-2.5 with 37 beamlet opertures.[7, 10]

thrust, µN	50	100	200	300	400	500	575
opt. positive high voltage, kV beam current, mA	0.372 1.56	0.791 2.18	1.079 3.74	1.334 5.06	1.571 6.22	1.806 7.26	1.980 7.98
rf-generator power, W total power input, W	12.4 13.1	13.3 15.2	14.9 19.2	16.0 21.6	16.9 27.0	17.7 31.2	18.25 34.4
total gas flow rate, sccm specific impulse, s	0.148 363	0.159 713	0.174 1236	0.186 1735	0.196 2194	0.206 2609	0.216 2861
propellant efficiency, % power efficiency, %	14.7 4.2	20.1 11.7	29.9 21.6	37.9 29.9	44.2 36.8	49.1 42.6	51.5 46.5

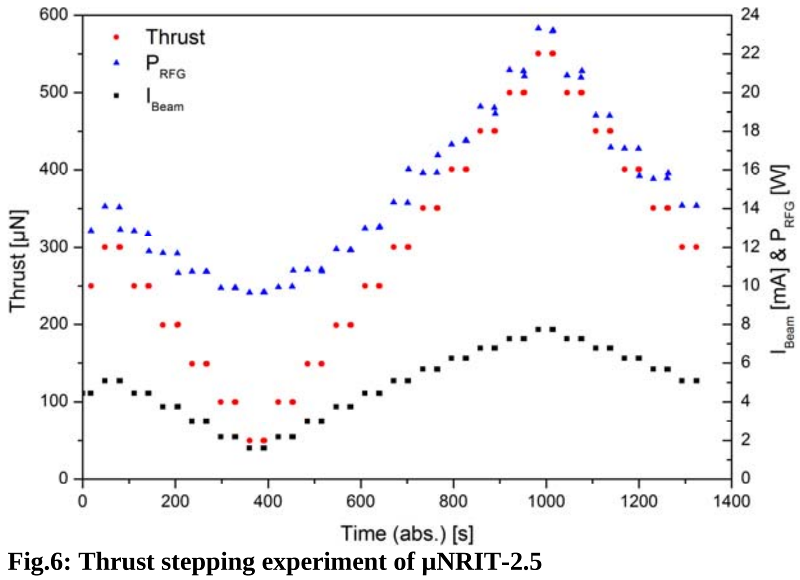

Fig.6: Thrust stepping experiment of µNRIT-2.5

To get the data of Table 3, the vertex values of each IBeam ($P_{RFG}, \dot{V}$) hyperbola and the beam voltages U_{PHV} with the minimum accel drain currents have been used.[7, 10]

The table shows that with strongly increasing thrust and U_{PHV} plus IBeam data, the rf-power and propellant flow requirements rise rather moderately. Therefore, both the power and propellant efficiency as well as the specific impulse increase strongly with the thrust.

At the *maximum measured thrust* of 575µN, η_m and η_e are around 50%, each, and the specific impulse approaches the 3000s-mark. On principle, the µNRIT-2.5 thrust could be further increased as the 8mA of beam current means a current density at the screen grid of (only) 7.63mA/cm^2 whereas the large RIT-22 is running with j_i = 11.83mA/cm^2 and U_{PHV} = 2.1 kV at nominal thrust. However, thermal problems with the 2.5cm laboratory microthruster prevent a continuous operation with 600µN or more.

The *minimum measured thrust* of 50µN shows such a poor performance in η_e, η_m and I_{sp}, that an µNRIT-2.5 operation underneath about 150µN would be quite ineffective.

To make accessible the ultrafine thrusting range, the number of beamlet apertures of the 2.5cm rf-microthruster could be reduced from 37 to 19,7 or even 1 (see Table 4). In this case P_{RFG}, η_m and I_{sp} would be constant, whereas IBeam and η_e are decreasing proportionally.

Table 3: Performance Range of µNRIT-2.5 for reduced number of beamlet apertures

number of beamlets	37	19	7	1
thrust range, µN	200-500	103-257	38-95	5.4-13.5
positive high voltage, kV beam current, mA	1.08-1.81 3.74-7.26	1.08-1.81 1.92-3.73	1.08-1.81 0.71-1.37	1.08-1.81 0.10-0.20
rf-generator power, W total power input, W	14.9-17.7 19.2-31.2	14.9-17.7 17.0-24.5	14.9-17.7 15.7-20.2	14.9-17.7 15.0-18.1
total gas flow rate, sccm specific impulse, s	0.174-0.206 1236-2609	0.089-0.106 1236-2609	0.033-0.039 1236-2609	0.0047-0.0056 1236-2609
propellant efficiency, % power efficiency, %	29.9-49.1 21.6-42.6	29.9-49.1 12.2-27.6	29.9-49.1 4.9-12.3	29.9-49.1 0.73-2.0

VI. Conclusion and Outlook

The Giessen laboratory prototype µNRIT-2.5 proved already performance data that are adequate for fine-thrusting applications.

The relatively low power consumption of a single microthruster enables the simultaneous operation of eight 500µN-engine with 250W. Another advantage is the small thruster mass of 210g, which means a total mass of 16 microthrusters of 3.36kg.

During the reported test campaigns, the engine was operated for 1200 hrs in total.

The further R & D work will be concentrated on the following topics:

1. A constructive revision should solve the thermal problems at high-thrust operation. Furthermore, the fixing system of the grid system may be redesigned for some mass savings.
2. The rf-generator including the rf-matching should be improved to operate the engine more effectively and at higher frequencies than 2.9MHz.
3. Rf-plasma and beam diagnostics should be carried out.
4. Performance mapping of the 2.5cm engine with reduced number of beamlets should be done.
5. A lifetest (with a closed decel grid) should be carried out.
6. A test with two microthrusters running simultaneously and feeded by one single RFG is envisaged.

Acknowledgments

The work has been supported by the German Aerospace Centre DLR at Bonn which is gratefully acknowledged.

List of Figures

Fig.1: Photo of the 2.5cm rf-microthruster µNRIT-2.5 of Giessen University.[7, 10]
Fig.2: Microthruster µNRIT-2.5 installed on a test platform in the facility “Big Mac”.[7, 10]
Fig.3: Extracted beam current (2mA to 8mA as the parameter) of µNRIT-2.5 as function of the

required rf-generator power PRFG and the propellant flow rate MFC.[7, 10]

List of Tables

References

1. F.M. Trojan, K.E. Bussweiler, H.H. Lang and H.W. Loeb: "Development of the Radio Frequency Thruster RIT-4", AIAA 72-473, Intern. Electric Prop. Conf., Bethesda 1972
2. H. W. Loeb, K. -H. Schartner, St. Weis, D. Feili and B. Meyer: "Development of RIT-Microthrusters", IAC-04-S.4.04, IAF-Congress, Vancouver 2004
3. D. Di Cara and M. Orlandi: "Micro-Newton RIT-4 Operational-Characterization Test, Test Report", TEC-MP/2006/246/DDC, Noordwijk 2006
4. EADS Endpräsentation July2009
5. O. Weller: "Bestimmung von Plasmaparametern in der RF-Entladung eines µ-Newton Triebwerks vom Typ RIT (µN-RIT) mittels einer Langmuir-Sonde", Diploma Thesis, Giessen 2009
6. D. Feili, H.W. Loeb, K.-H. Schartner, St. Weis, D. Kirmse and B. Meyer: "Performance Mapping of New µN-RITs at Giessen", IEPC-2005-252, 29th Intern. Electric Prop. Conf., Princeton 2005
7. B. Lotz: "Design, Konstruktion und Test eines entladungsoptimierten Ionenstrahltriebwerks des RIT-Typs", Diploma Thesis, Giessen 2009
8. H.W. Loeb, J. Freisinger, K.H. Groh and A. Scharmann: "State-of-the-Art of the RIT-Ion Thrusters and Their Spin-Offs", IAF-88-258, 39th IAF-Congress, Bangalore 1988
9. H. W. Loeb, K. -H. Schartner, D. Feili, H.-P. Harmann, H. Bassner, R. Killinger, H. Leiter and J. Mueller: "Recent Investigations, Development and Industrial Applications of Rf-Ion Thrusters in Germany", IAC-02-S.4.06, 53rd IAF-Congress, Houston 2002
10. H.W. Loeb, D. Feili and B. Lotz: "RIT-2.5- A New Optimized Microthruster of Giessen University", Technical Note Giessen 2009
11. H. Leiter and D. Feili: "Rit-15s- A Radio-Frequency Ion Engine for High Specific Impulse Operation", 37th Joint Propulsion Conf., Salt Lake City 2001